BBA - Gene Regulatory Mechanisms 1866 (2023) 194901

Contents lists available at ScienceDirect

BBA - Gene Regulatory Mechanisms

journal homepage: www.elsevier.com/locate/bbagrm

OTUD3: A Lys6 and Lys63 specific deubiquitinase in early vertebrate development☆

Florian Job [a,b,1], Carolin Mai [a,1], Pablo Villavicencio-Lorini [b], Juliane Herfurth [a], Herbert Neuhaus [a], Katrin Hoffmann [b], Thorsten Pfirrmann [a,c], Thomas Hollemann [a,*]

[a] Martin-Luther-University Halle-Wittenberg, Institute for Physiological Chemistry, 06114 Halle, Germany
[b] Martin-Luther-University Halle-Wittenberg, Institute of Human Genetics, 06114 Halle, Germany
[c] Department of Medicine, Health and Medical University, 14471 Potsdam, Germany

ARTICLE INFO

Keywords:
OTUD3
Deubiquitinase
Ubiquitin
Proteasome
Neural crest
Xenopus

ABSTRACT

Ubiquitination and deubiquitylation regulate essential cellular processes and involve hundreds of sequentially acting enzymes, many of which are barely understood. OTUD3 is an evolutionarily highly conserved deubiquitinase involved in many aspects of cellular homeostasis. However, its biochemical properties and physiological role during development are poorly understood. Here, we report on the expression of OTUD3 in human tissue samples where it appears prominently in those of neuronal origin. In cells, OTUD3 is present in the cytoplasm where it can bind to microtubules. Interestingly, we found that OTUD3 cleaves preferentially at K6 and K63, i.e., poly-ubiquitin linkages that are not primarily involved in protein degradation. We employed *Xenopus* embryos to study the consequences of suppressing *otud3* function during early neural development. We found that Otud3 deficiency led to impaired formation of cranial and particularly of cranial neural crest-derived structures as well as movement defects. Thus, OTUD3 appears as a neuronally enriched deubiquitinase that is involved in the proper development of the neural system.

1. Introduction

Ubiquitination is a posttranslational modification that regulates many cellular processes including proteolysis, cell proliferation, macromolecule trafficking, DNA damage repair, receptor signaling, cell communication and immunologic recognition processes [1–3]. Conjugation of ubiquitin via the formation of an isopeptide bond between the C terminus of ubiquitin and a lysine residue of a substrate protein requires the activity of ubiquitin writers (three sequentially acting enzymes including E3 ubiquitin ligases) [4–7]. The action of E3 ubiquitin ligases is opposed by deubiquitinating enzymes (DUBs) called erasers. The human genome encodes for approximately 100 DUBs, which can be sorted into six groups: ubiquitin specific proteases (USPs), ubiquitin C-terminal hydrolases (UCHs), ovarian tumor proteases (OTUs), Machado-Joseph disease protein domain proteases (JMD), JAB1/MPN/MOV34 metalloenzymes (JAMM/MPN+), and monocyte chemotactic protein-induced proteins (MCPIP) [8–10]. Members of the USP family (56 proteins) are promiscuous for different ubiquitin linkage topologies, whereas members of the OTU family are selective for different types of ubiquitin chains [11–13]. Ubiquitin moieties can be linked via seven internal lysine residues (K6, K11, K27, K29, K33, K48, K63) forming ε-amines (Lys-linked ubiquitination) and the N-terminal methionine (Met1-linked ubiquitination). Substrates can remain mono-ubiquitinylated or are mono-ubiquitinylated at multiple sites [14]. They can receive homotypic polyubiquitin chains (containing only one linkage type) or branched polyubiquitin chains of defined linkage types. Several lysines of ubiquitin can become modified post-translationally, e.g., by acetylation or phosphorylation which can inhibit chain elongation [15–17]. However, each event initiates a distinct signaling sequence based on the specific structural quality they represent in the cell.

Nine core OTUD genes exist in humans, and we have only begun to understand their functions. Among them, OTUD1 stabilizes PTEN as well as p53 protein and reverse K63-linked ubiquitination of YAP as well as the K6-linked ubiquitination of IRF3 [18–21]; OTUD2/YOD1 acts as

☆ Special issue on "The ubiquitin system"; Edited by Hai Rao, Michael Glickman, Feng Rao.

* Corresponding author.
E-mail address: thomas.hollemann@medizin.uni-halle.de (T. Hollemann).

[1] These authors contributed equally to this work.

https://doi.org/10.1016/j.bbagrm.2022.194901
Received 27 September 2022; Received in revised form 17 November 2022; Accepted 29 November 2022
Available online 9 December 2022

antagonist of TRAF6 signaling to NF-kB and is involved in NEDD4-dependent Hippo-signaling [22,23]. OTUD3 is described as a tumor suppressor that can act as a K48-specific deubiquitinase and stabilizes PTEN as well as reverse K63-linked ubiquitination of MyD88 and TP53. High expression of OTUD3 correlates with poorer survival of lung cancer patients while *Otud3* deficiency promotes breast cancer formation in mice. Recently, OTUD3 has also been described to affect innate immunity [24–32]. Since suppression of OTUD4 function in zebrafish leads to defects in neural development and enhances TGFbeta signaling, it serves as a predictive marker in several cancers [26,33,34]. OTUD5/DUBA is a negative regulator of interferon and interleukin production of immune responses and stabilizes p53 [35–37]. More recent data have shown that OTUD5 is involved in the response to DNA damage and cancer progression [37–41]. Mutations in *OTUD6B* have been shown to result in seizures and impaired development of facies and distal limbs as well as intellectual and visual disabilities [42,43]. The loss of Otud6b in mice leads to the death of homozygous embryos due to reduced cell proliferation and heart defects [44]. OTUD7A (Cezanne-2) and OTUD7B (Cezanne), like OTUD2, are involved in antagonizing TRAF6 activity with OTUD7A suppressing migration and invasion of HCC cells [45–47]. *Otud7a* transcription is repressed by SNAIL1, an important transcription factor for neural crest migration and specification. Moreover, two publications describe the deletion in OTUD7A as causal for neurological defects of the 15q13.3 microdeletion syndrome [48–51]. OTUD7B is involved in HIF-1a homeostasis and is therefore a regulator of hypoxia. Furthermore, it functions in autophagy as well as in the inflammation of endothelial cells [52–55].

Here, we report on the biochemical and cellular properties of OTUD3 in cell culture. Moreover, since the role of OTUD3 during early development has not been examined so far, we used the African clawed frog *Xenopus laevis* as a vertebrate model organism. *Xenopus* develops extrauterine and thus independently from maternal influences. We found that suppression of *otud3* leads to impaired formation of cranial and cranial neural crest-derived structures, leading to movement defects in the tadpole.

2. Materials and methods

2.1. Plasmids, antibodies, primer, and chemicals

Description of plasmids, antibodies, and primers can be found in the Supplementary material. Unless stated otherwise, all drugs and chemicals were purchased from Roth GmbH, Karlsruhe, Germany.

2.2. Cultivation of cells and transfections

Primary fibroblasts were cultivated in DMEM/HamsF12 (1:1) (Gibco) medium supplemented with 8 % FCS (GE Healthcare, Braunschweig, Germany), 2 % Ultroser G (Cytogen, Wetzlar, Germany), and 2 mM glutamine (PAA). HT22 cells were cultivated in DMEM supplemented with 10 % FCS and 2 mM glutamine. Transfections of plasmids were performed using Lipofectamine 2000 (Invitrogen, Carlsbad, CA, USA) according to the manufacturer's protocol. Empty vector pCS2^{+} was used to obtain equal amounts of transfected DNA and as a negative (EV) control. Cells were harvested 48 h after transfection or analyzed by immunofluorescence microscopy. To block polymerization of microtubules, 10 μM nocodazole suspended in DMSO (Sigma-Aldrich, Darmstadt, Germany) was added to the cells.

2.3. OTUD3 activity and specificity assays

For the activity assays, HEK293T and SH-SY5Y were seeded into six-well plates and allowed to grow to 70–80 % confluency. Cells were transfected with different GFP-OTUD3 variants using Lipofectamine 2000 or PEI according to the manufacturer's instructions and incubated for 24 h. Cells were harvested by adding 300 μl of Trypsin/EDTA (PAA) to each well. After 5 min, cells were suspended in 3 ml cultivation medium and centrifuged (3 min at 1500 rpm). Cell pellets were washed once with 3 ml PBS and lysed in 20 mM Tris (pH 8.0), 100 mM NaCl, 1 mM EDTA, 0.5 % Triton-X100 and freshly added 1 mM PMSF, 1 mM Aprotinin, 50 μM MG132, 1 mM DTT, and 2 mM ATP for 30 min on ice. After centrifugation at 13,000 rpm at 4 °C for 10 min, the supernatant was transferred to a new tube. 20 μg of each cell lysate was incubated for 1 h at 37 °C with or without 1 μg ubiquitin-propargylamide (Ub-PA, Boston Biochem, Cambridge, MA, USA) or ubiquitin-vinylmethylester (Ub-VME, Boston Biochem, Cambridge, MA, USA). In addition, 10 mM of N-ethylmaleimide (NEM, Sigma-Aldrich, Darmstadt, Germany) was added 15 min prior to ubiquitin-substrates. Reactions were stopped by adding SDS loading buffer containing 5 % (v/v) 2-mercaptoethanol and heating to 95 °C for 10 min. Samples were separated on 4–12 % Tris-glycine gels (Invitrogen, Thermofisher, Waltham, MA, USA) for 90 min at 140 V and subsequently transferred onto PVDF membranes for 70 min at 100 V. Membranes were blocked for 1 h at room temperature in TBS, 0.05 % Tween-20 (TBST), and 5 % (w/v) milk powder. Primary anti-OTUD3 antibody (monoclonal mouse, Millipore clone 12A6.1; MABS1819) was diluted 1:1000 in TBST and 0.5 % (w/v) milk powder and used for membrane incubation overnight at 4 °C. Membranes were washed (3 × 10 min in TBST) and secondary HRP-coupled anti-mouse IgG (1:10,000) in TBST was applied for 1 h at room temperature. After washing, an ECL plus Western blot detection Kit (Pierce, Thermofisher, Waltham, MA, USA) was used according to the manufacturer's protocol. Membranes were blotted with anti-GAPDH antibodies as loading controls (1:5000, monoclonal mouse; Sigma; G8795). For the specificity assays, a mutant HEK293T clone, lacking endogenous OTUD3 expression, was used. Cells were seeded onto 10 cm cell culture dishes, grown to 70–80 % confluency, and transfected with 10 μg of different GFP-tacked OTUD3 variants. After 24 h, cells were washed with ice cold PBS and harvested using 200 μl RIPA buffer (25 mM Tris-HCl pH 7.4; 150 mM NaCl; 2 mM EDTA; 1 % Triton X-100; 0,1 % SDS; +cComplete, EDTA free) on ice. Lysates were scraped off and transferred to Eppendorf tubes, incubated for 30 min on ice, and mixed every 10 min by pipetting up and down. Lysates were centrifuged with 17,000 ×*g* at 4 °C for 10 min and supernatants were transferred to new pre-cooled tubes. 300 μl dilution buffer (10 mM Tris-HCl pH 7.5; 150 mM NaCl; 0.5 mM EDTA) was added to the lysates. GFP trap beads (Chromotek) were added to the lysates according to the manufacturer's instructions and incubated for 1 h on a rotating wheel at 4 °C. The beads were centrifuged for 5 min with 2500 ×*g* at 4 °C and washed three times in 500 μl washing buffer (10 mM Tris-HCl pH 7.5; 150 mM NaCl; 0.5 mM EDTA; 0.05 % NP-40). After the last washing cycle, 50 μl of 10× DUB-buffer (500 mM Tris-HCl pH 7.5; 500 mM NaCl; 50 mM DTT) were added. 30 μl of the purified OTUD3 proteins were incubated with 2 μg of tetra-Ubiquitin chains for 30 min at 37 °C. The reactions were terminated by adding 10 μl of 4× LDS sample buffer (Alfa Aesar) including 100 mM DTT. Probes were heated to 95 °C for 5 min, separated on 10–20 % Tris-Glycine gels, and silver stained using the Invitrogen SilverQuest Staining Kit.

2.4. Immunofluorescence microscopy

Primary fibroblasts were grown on polylysine coated glass plates in 12-well plates under standard conditions. Cells were washed twice with PBS and then fixed in 4 % paraformaldehyde for 30 min at 4 °C and permeabilized in PBS containing 0.2 % Triton X-100 for 5 min at 4 °C, subsequently washed (3 × 10 min PBS) and incubated in PBS and 2 % BSA for 30 min. Slides were decorated firstly with anti-OTUD3 (1:100, Novus Biologicals, Wiesbaden, Germany) and secondly with IgG Alexa488 (1:200, Invitrogen, Carlsbad, CA, USA). DNA was stained with DAPI.

2.5. RNA extraction from human cell culture and Xenopus embryos

RNA was isolated from 25cm^2 of confluent fibroblast cultures using

RNeasy Mini Kit (QIAGEN) according to the manufacturer's protocol. RNA from frozen, staged *Xenopus* embryos was isolated as described previously [56]. RNA was subsequently used for cDNA synthesis or stored at −80 °C for further processing.

2.6. cDNA synthesis and quantitative PCR

OTUD3 mRNA levels were analyzed in primary fibroblasts and a panel of 18 human tissues (Stratagene, San Diego, CA, USA) by quantitative PCR (qPCR). Total RNA (1 μg) was reverse transcribed into cDNA in a 20 μl reaction using random hexamer primers and a ProtoScript cDNA synthesis Kit. A 20 μl qPCR reaction contained 10 ng cDNA, 1xHOT FIREPol® EvaGreen® qPCR Mix Plus (passive reference ROX, Solis Biodyne, Tartu, Estonia), and 1.25 μM of primers. The following intron-spanning RT-PCR primer pairs (Suppl. table S3) were used: *OTUD3*-F + R: (fragment size: 90 bp); *GAPDH*-F + R: (endogenous control; fragment size: 87 bp) *OTUD3*, and *GAPDH* primer pair efficiency was controlled in a standard template dilution experiment and found to be similar (*OTUD3*: 96.7 %; *GAPDH*: 98.2 %). The qPCR protocol consisted of a 15 min hot start at 95 °C, followed by 36 cycles consisting of a 20s denaturation step at 95 °C, a 30s annealing step at 55 °C, and a 20s extension step at 72 °C, running PCR on a StepOnePlus instrument (ABI, Thermofisher, Waltham, MA, USA). After amplification, samples were heated for 30s at 95 °C, cooled for 30s at 65 °C, then heated again to 95 °C while measuring fluorescence every 0.3 °C to generate melting curves to confirm homogeneity of the generated PCR product. Relative expression was determined using the $2^{-\Delta\Delta}$Ct method [57] and the StepOnePlus software (ABI, Thermofisher, Waltham, MA, USA). For the analyses of *OTUD3* mRNA levels in fibroblasts, data were collected in triplicate from three independent experiments and presented as mean ± SEM.

2.7. cDNA synthesis and semi-quantitative RT-PCR of Xenopus embryos

Levels of *otud3* mRNA in *Xenopus* embryos of consecutive developmental stages were measured by semi-quantitative RT-PCR. Total RNA (1 μg) was reverse transcribed into cDNA in a 20 μl reaction using random hexamer primers and ProtoScript cDNA synthesis Kit (Sigma-Aldrich, Darmstadt, Germany). A 25 μl qPCR reaction contained 10 g cDNA, 1× HOT FIREPol® and 0.4 μM primers. The following RT-PCR primer pairs (Suppl. table S3) were used: *otud3* (fragment size: 230 bp), *odc1* (fragment size: 220 bp), and *p53* (fragment size: 248 bp).

2.8. Animals, microinjections, and animal cap explants

Xenopus laevis were obtained from NASCO, Fort Atkinson, WI, USA. Embryos were generated and cultured as described [58]. Staging was according to Nieuwkoop and Faber [59]. All procedures were performed according to guidelines set by German animal use and care laws (Tierschutzgesetz) and approved by the German state administration of Saxony-Anhalt (Projekt/AZ: 42502-3-600 MLU). For loss-of-function experiments, two antisense morpholino-oligonucleotides (*otud3*-mo1/2) were designed and ordered from GeneTools, Philomath, Oregon, CA, USA. For control injections, the standard control morpholino from Gene Tools (Philomath, Oregon, CA, USA) was used. Sequences are listed in the Supplementary Table S1. All morpholinos were dissolved in DEPC-H_2O and stored in aliquots at −80 °C. For all experiments, 2.5 pmol of the morpholinos or 1 ng of synthetic RNA was injected unilaterally into one blastomere at the two-cell stage. Synthetic *beta-gal* RNA (100 pg) was co-injected as a lineage tracer in all experiments. Synthetically capped RNA was generated using the mMESSAGE mMACHINE kit (Ambion, Thermofisher, Waltham, MA, USA). *Not*I linearized $pCS2^+$ containing the gene of interest was used as a template for SP6 transcription and 5 nl of capped mRNA were injected along with the morpholino into one blastomere of a 2-cell stage embryo. The non-injected side served as internal control.

2.9. Cloning

Full-length *Xenopus laevis otud3* was amplified by reverse transcriptase PCR using primer pair *otud3*-F1 and *otud3*-R, bluntly ligated into pGEM-T and subcloned into the *Eco*RI-*Xho*I site of $pCS2^+$ to generate $pCS2^+$:*otud3*. Full-length *Homo sapiens OTUD3* was subcloned into the *Eco*RI-*Xho*I site of $pCS2^+$ to generate $pCS2^+$:*OTUD3* using plasmid GFP-*OTUD3* as template (*OTUD3*-F1 and *OTUD3*-F as primers) [60]. Translation of constructs was controlled by couple transcription and translation (data not shown) (Promega, San Luis Obispo, CA, USA).

2.10. Whole-mount in situ hybridization

Whole-mount in situ hybridization (Wmish) experiments were carried out as described previously [61]. To generate antisense RNA probes, corresponding plasmids were digested and transcribed using standard protocols for *pax6*, *n-tubulin*, *twist*, *sox10*, and *foxd3*. After embedding embryos in gelatin/albumin, 10 μm sections were prepared using a microtome (Leica, Nussloch, Germany) and mounted on glass slides.

2.11. Alcian blue staining

Cartilage staining in *Xenopus laevis* embryos was performed as described earlier [62]. In brief, embryos were fixed in MEMFA at NF stage 45 for 2 h at room temperature. Afterwards, embryos were rinsed in PBS and stained with 1 % Alcian blue containing 0.5 % acetic acid for 2 h at room temperature. Staining solution was removed and embryos were maintained in 80 % ethanol/20 % acetic acid. For bleaching, embryos were first incubated for 3 h in 30 % H_2O_2 and an additional 2 h in 0.05 % Trypsin in a saturated sodium tetraborate solution. After PBST rinsing for several days at 4 °C, the skin of the embryos was removed, and regions of interest were photographed.

3. Results

3.1. OTUD3 is highly conserved in evolution

Prominent features of the OTUD3 protein include the catalytic OTU domain and the ubiquitin-associated (UBA) domain. The OTU domain contains conserved cysteine, aspartate, and histidine residues that compose the catalytic triad of a cysteine protease. The UBA domain is a short sequence motif composed of a compact three-helix bundle with a large hydrophobic surface patch. UBA domains bind ubiquitin as well as other proteins lacking any obvious ubiquitin-like structure [63,64]. To date, specific functions of the N- and C-terminal region of OTUD3 have not been determined, largely because structural data for these regions is missing. The amino acid sequence alignment of OTUD3 revealed a high degree of conservation throughout the eukaryotic kingdom. To analyze the extent of OTUD3 conservation, we compared OTUD3 sequences from 16 eukaryotic organisms representing seven classes: *Echinoidea* (*Strongylocentrotus purpuratus*; purple sea urchin), *Bivalvia* (*Crassostrea gigas*; Pacific oyster), *Leptocardii* (*Branchiostoma belcheri*; lancelets), *Actinopterygii* (*Danio rerio*, *Takifugu rubripes*; ray-finned fishes), *Amphibia* (*Xenopus tropicalis*, *Xenopus laevis*; claw frogs), *Aves* (*Corvus japonica*, *Gallus gallus*; birds), and *Mammalia* (*Monodelphis domestica*, *Ornithorhynchus cuniculus*, *Rattus norvegicus*, *Mus musculus*, *Mesocricetus auratus*, *Pan troglodytes*, *Homo sapiens*; Fig. 1A, B).

Furthermore, vertebrate synteny analysis demonstrated a high degree of similarity in the genomic arrangements of *OTUD3* (Fig. 1C). BLAST analysis also confirmed the mostly conserved genomic arrangement of gene loci close to *OTUD3*. Genes encoding HTR6, TMCO4, and RNF186 were frequently located downstream of OTUD3, whereas upstream of OTUD3 a linear arrangement of numerous PLA2 genes was present. A less conserved gene arrangement was observed only in zebrafish. These findings show that OTUD3 is highly conserved during evolution which may indicate an important cellular function.

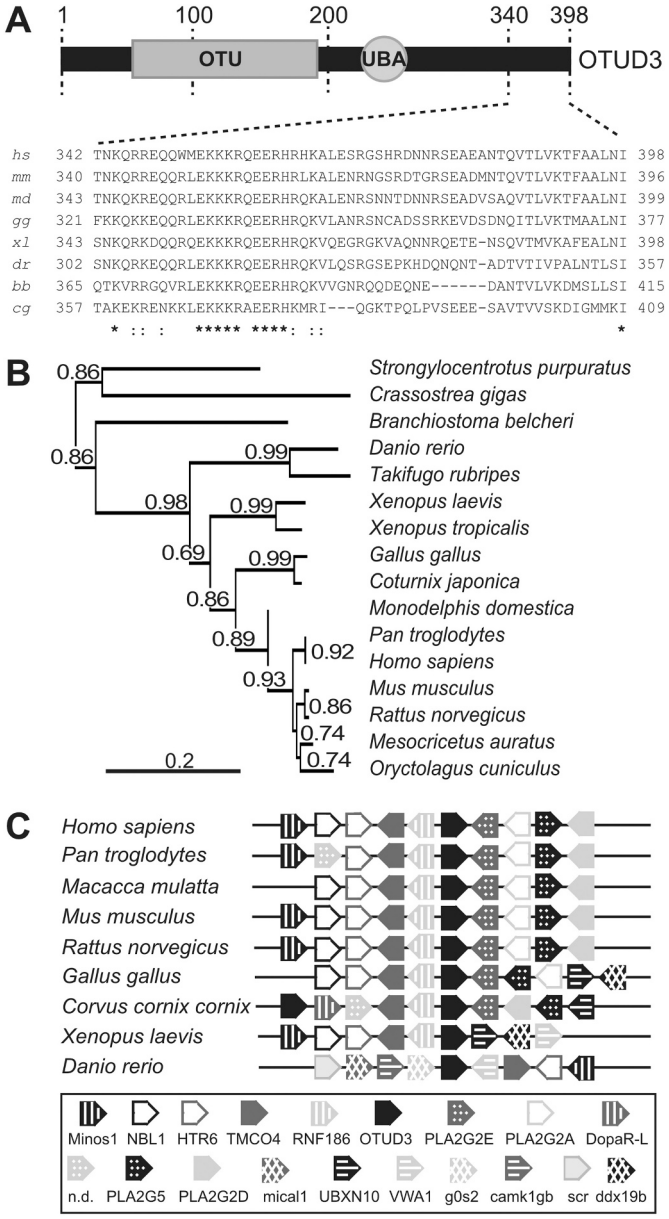

Fig. 1. OTUD3 is highly conserved in evolution. A) OTUD3 protein contains an OTU domain bearing a putative cysteine protease and an UBA interaction site. Of note is a characteristic isoleucine forming the last amino acid of the protein. B) Phylogenetic tree of putative full-length OTUD3 selected from the animal kingdom based on maximum likelihood and bootstrap analysis. The branch length is proportional to the number of substitutions per site. The numbers next to the nodes are bootstrap support values. Branch lengths are scaled based on the estimated divergence, with the scale bar at the bottom of the phylogram indicating the evolutionary distance. There is a 20 % relative divergence observed over time. Notably, mammals, birds, fishes, and amphibians show a close phylogenetic lineage. C) Synteny analysis of *OTUD3/otud3*: The location and orientation of *OTUD3/otud3* in the respective genomes is conserved. Each arrow stands for a single gene while the arrowhead indicates the direction of the open reading frame (ORF). *OTUD3/otud3* (black arrow) is present in all analyzed species. In all species except zebrafish, up- and downstream *OTUD3/otud3* is flanked by the same genes. Abbreviations: GenBank Accession numbers, GBA-no.; *bb*, *Branchiostoma belcheri* (lancelets), GBA-no. XM_019782191; *cg*, *Crassostrea gigas* (Pacific oyster), GBA-no. XM_011447637; *Coturnix japonica* (Japanese quail), GBA-no. XM_015882304; *dr*, *Danio rerio* (zebrafish), GBA-no. NM_212922; *gg*, *Gallus gallus* (domestic chicken), GBA-no. XM_424363; *hs*, *Homo sapiens*, GBA-no. NM_015207; *Mesocricetus auratus* (golden hamster), GBA-no. XM_005081047; *md*, *Monodelphis domestica* (opossum), GBA-no. XM_001377743; *mm*, *Mus musculus* (house mouse), GBA-no. NM_028453; *Oryctolagus cuniculus* (common rabbit), GBA-no. XM_002716005; *Pan troglodytes* (common chimpanzee), GBA-no. XM_513073; *Rattus norvegicus* (common rat), GBA-no. NM_001191983; *sp*, *Strongylocentrotus purpuratus* (purple sea urchin), GBA-no. XM_001191596; *Takifugo rubripes* (pufferfish), GBA-no. XM_003962965; *xl*, *Xenopus laevis* (African claw frog), GBA-no. NM_001095317; *xt*, *Xenopus tropicalis* (Western claw frog), GBA-no. NM_001005056.

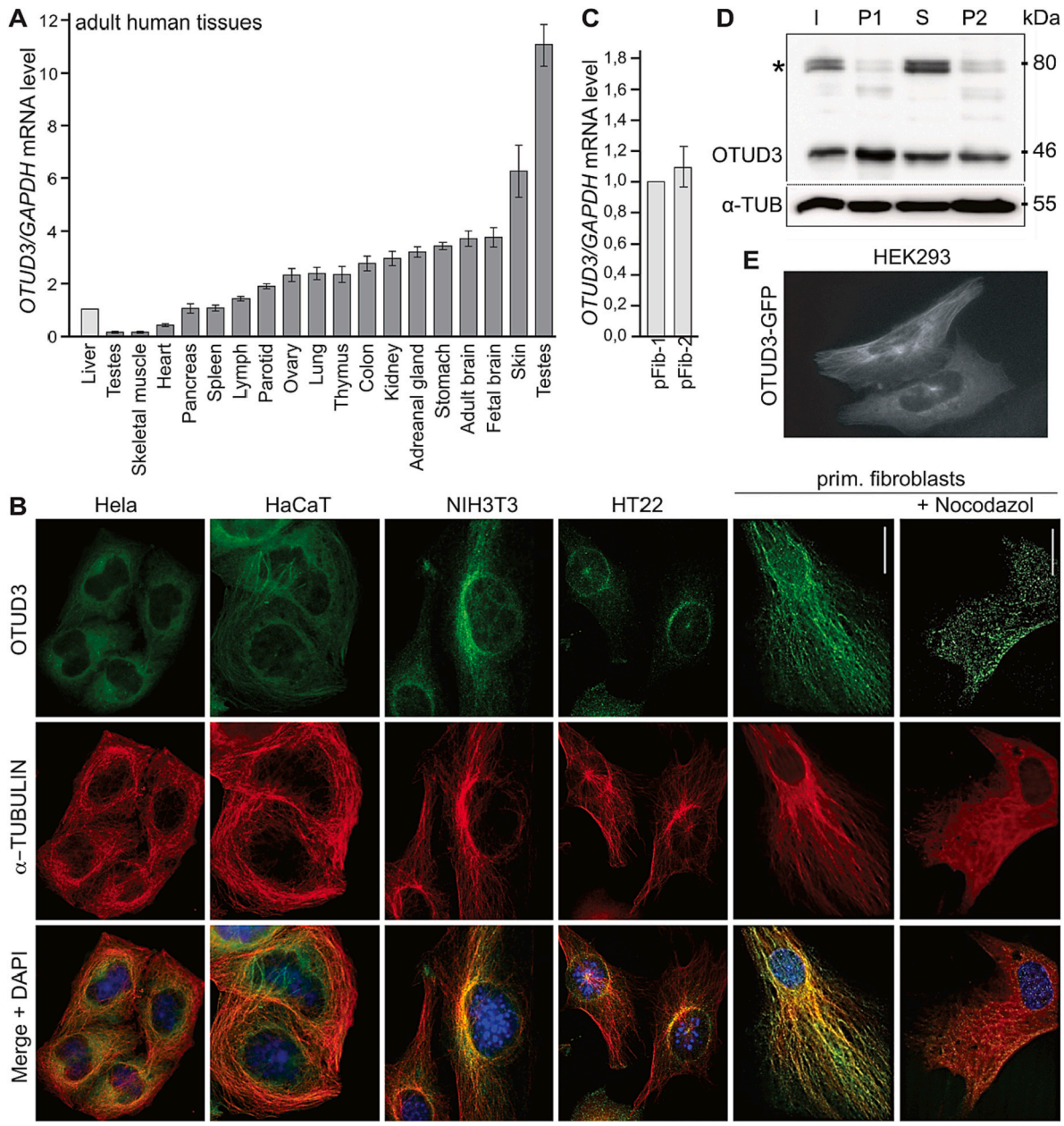

Fig. 2. Analysis of OTUD3 expression. (A) Relative transcript levels of *OTUD3* mRNA in total RNA preparations from adult human tissues (BD Biosciences Clontech). *OTUD3* mRNA levels were normalized to expression level of human liver. *OTUD3* mRNA was detected in all tissues investigated. Highest levels of *OTUD3* mRNA were measured in testes and skin. Notably, strong expression was found in adult and fetal brain. (B) OTUD3 in several human and mouse cell lines localized mainly in cytosol and, to a lesser extent, into the nucleus. HeLa: human malignant epithelial cells; HaCaT: human aneuploid immortal keratinocytes; NIH3T3: mouse embryonic fibroblasts; HT22: mouse hippocampal neuronal cells; pFib: human primary fibroblasts. Nuclear DNA was stained with DAPI (blue). Note the prominent co-staining of OTUD3 and alpha-TUBULIN, which, upon treatment with nocodazole, was strongly reduced in primary fibroblasts. (C) Relative *OTUD3* transcript levels in primary fibroblasts measured by quantitative PCR. OTUD3 was present in polymerized tubulin fraction. Wildtype OTUD3 was overexpressed in HeLa cells. (D) By differential ultra-centrifugation, cell lysates (I) were fractionated into a nuclear/debris fraction (P1), a soluble (S), and an insoluble pellet fraction (P2). Samples of each fraction were loaded on SDS PAGE gel. Western blot was performed applying anti-OTUD3 antibody (Novus Biologicals, 1:200). Anti-α-tubulin antibody (Sigma, 1:500) was used as loading control. (E) Transfection of HEK293T cells with a plasmid encoding an OTUD3-GFP fusion protein also indicates the association of OTUD3 with tubulin filaments. (For interpretation of the references to color in this figure legend, the reader is referred to the web version of this article.)

3.2. OTUD3 is highly expressed in neuronal tissues and co-localizes with microtubules

We investigated the expression pattern of *OTUD3* by RT-qPCR using an RNA panel from 18 human tissues (Fig. 2A). *OTUD3* expression was highest in skin and testes with remarkably high *OTUD3* mRNA levels in fetal and adult brain tissue. Moreover, using immunofluorescence microscopy we found OTUD3 expression in all investigated human and mouse cell lines, namely in human malignant epithelial cells (HeLa), human aneuploid immortal keratinocytes (HaCaT), mouse embryonic fibroblasts (NIH3T3), mouse hippocampal neuronal cells (HT22), and in human primary fibroblasts (pFib). To confirm the expression of OTUD3 in primary fibroblasts, we performed RT-qPCR in two independent cell lines (Fig. 2B, C). OTUD3 localized primarily to the cytosol with perinuclear accumulation and a minor fraction appeared in the cell nucleus. Comparing the alpha-TUBULIN and OTUD3 fluorescence signals, we noticed co-localization of endogenous OTUD3 with tubulin filaments, where OTUD3 signal is visualized as small dots. In the presence of

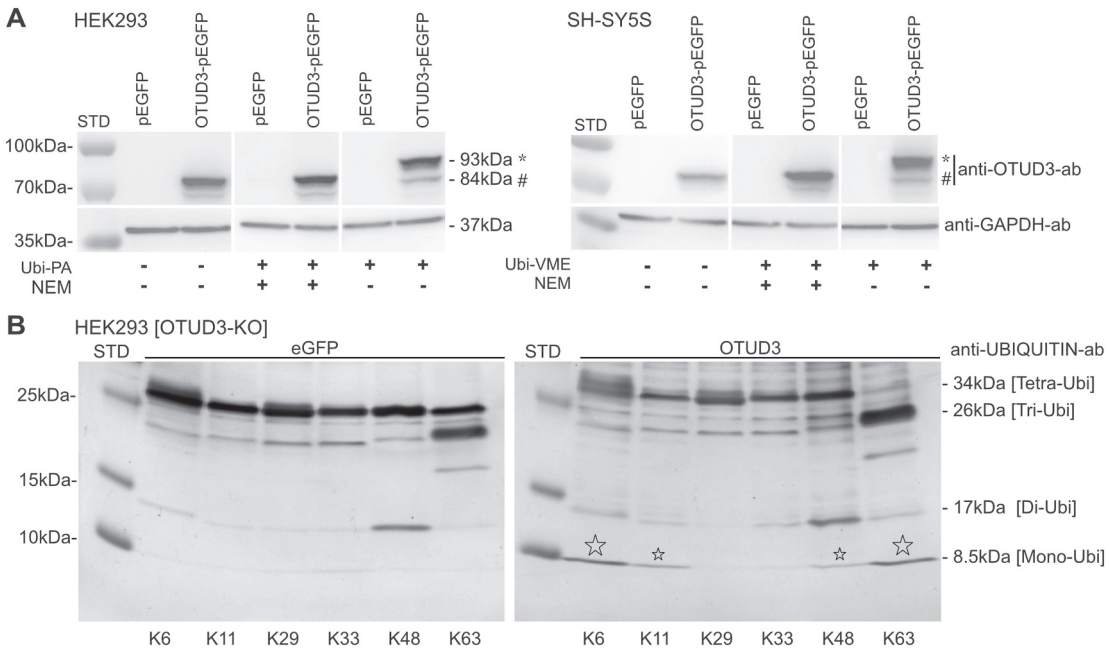

Fig. 3. OTUD3 catalytic activity and specificity. (A) The activity of OTUD3 cysteine protease function was measured upon transfection of cell lysates of HEK293T and SH-SY5Y with OTUD3-GFP (SH-SY5Y, Suppl. Fig. 1A; full western blots, Suppl. Fig. 1B). Cell lysates were incubated in the presence or absence of 1 μg ubiquitin-propargylamide protein (Ubi-PA) or ubiquitin-vinylmethylester (Ubi-VME). NEM was added to block protease activity to control specificity. An anti-GAPDH blot is shown as loading control. (B) OTUD3-KO cells (HEK293T) were transfected with either GFP or OTUD3-GFP. Tetra-ubiquitin chains of a defined linkage type were incubated with GFP-OTUD3 protein purified from cell lysates using a GFP trap method. After incubation for 30 min at 37 °C, the reactions were separated on denaturing gradient SDS polyacrylamide gel electrophoresis and silver stained.

nocodazole, a compound that interferes with polymerization of microtubules, we still noticed the small OTUD3-containing dots; however, the profound co-localization of OTUD3 with the microtubules was no longer present. The co-localization of OTUD3 and TUBULIN prompted us to investigate the biochemical interaction between OTUD3 and polymerized microtubules in a co-sedimentation assay (Fig. 2D). HeLa cells were transiently transfected with OTUD3, and lysed cells were fractionated into polymerized and unpolymerized tubulins by ultracentrifugation. By western blotting and applying anti-OTUD3 antibody we obtained the total cell lysate (I), a nuclear/debris fraction (P1), the fraction of unpolymerized/soluble tubulins (S), and the polymerized/insoluble/pellet microtubule fraction (P2). OTUD3 protein was detected in all separated cellular fractions. Thus, OTUD3 pelletized with polymerized microtubules, which, together with our immunofluorescence data, indicates an interaction of OTUD3 with microtubules. Since the transfection with N-terminally GFP-tagged OTUD3 resulted in the same localization of the GFP signal in the cytoplasm, mostly in a filament-like pattern, the commercial OTUD3 antibody appears to be specific (Fig. 2E). All further experiments were performed using OTUD3-GFP transfected cell lines. Thus, our experiments show that OTUD3 is expressed in all tissues or cell lines tested and interacts with microtubules in the cytoplasm. We conclude that OTUD3 is expressed in all cells but with a higher level in neuronal derived tissues. The interaction of OTUD3 with cellular microtubules and OTUD3 localization to the nucleus indicates a compartment specific regulation of OTUD3 activity via the retention of OTUD3 at the microtubules.

3.3. OTUD3 catalytic activity

The linkage type of ubiquitin chains provides specificity of the signal they can convey. It is therefore crucial to understand protease specificity and activity of a given deubiquitylating enzyme that can revert this ubiquitin-signal. We first investigated whether full-length OTUD3 can bind and process ubiquitin (Fig. 3) by employing human embryonic kidney cells (HEK293T), and a neuroblast-like subclone of a bone marrow biopsy (SH-SY5Y, Supplementary Fig. 1), and two suicide substrates (Ubi-PA: Ubiquitin-Propargylamide Protein and Ubi-VME: Ubiquitin-Vinyl Methyl Ester) which - upon catalysis - remain covalently bound to the active center OTUD3 after processing. Using NEM (N-ethylmaleinimid), an irreversible inhibitor of cysteine peptidases, to test for the specificity of both suicide substrates we found that both suicide substrates were unable to bind to OTUD3 with NEM present. In contrast, without NEM both modified ubiquitin bound to OTUD3 but could not be relieved from the active center, resulting in a mass shift by one ubiquitin moiety. Further, we tested the specificity and reactivity of OTUD3, and thus the mode of recognition and interaction, by adding linear polyubiquitin chains of a given linkage type.

To ensure that the observed chain cleavages did indeed result from OTUD3 activity, we transfected CRISPR/Cas-generated OTUD3 knockout cells (Supplementary Fig. 2) with plasmids of OTUD3-GFP or GFP. Also, we intended to introduce an enzymatically dead version of OTUD3 as a further specificity control, but all variants carrying a deletion of a defined critical amino acid of the catalytic tetrad induced cell death in all tested eukaryotic cell lines (Suppl. Fig. 1B), similar to what was reported previously [65]. Full-length OTUD3 preferentially cleaves K6 and K63 ubiquitin linkages (Fig. 3B) and to a lesser extent K11 and K48, while K29 and K33 were not cleaved at all. Thus, apart from withdrawing ubiquitinated proteins from degradation by the proteasome, OTUD3 likely possesses protein regulatory functions.

3.4. *Otud3* is required for the formation of the anterior axis in *Xenopus laevis*

The expression of OTUD3 in human adult and fetal brain and the high degree of conservation prompted us to investigate a possible role of OTUD3 during early *Xenopus* development. Firstly, we examined basal expression of *otud3* in consecutive developmental stages of *Xenopus laevis* by semi-quantitative RT-PCR. Analysis of *otud3* expression over time revealed high initial levels of maternal transcripts declining steadily until gastrulation. Zygotic transcripts were detectable

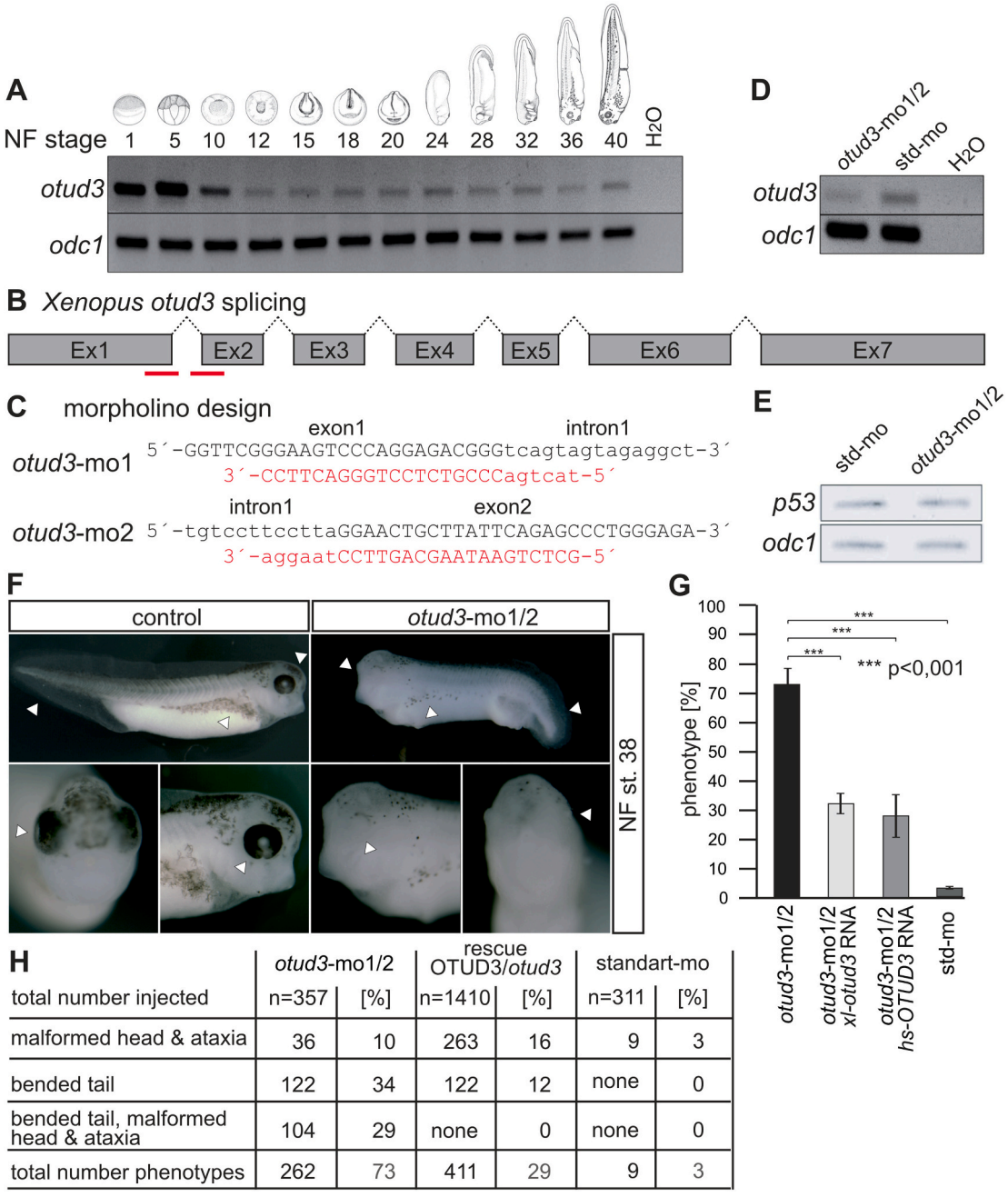

H

total number injected	otud3-mo1/2 n=357	[%]	rescue OTUD3/otud3 n=1410	[%]	standart-mo n=311	[%]
malformed head & ataxia	36	10	263	16	9	3
bended tail	122	34	122	12	none	0
bended tail, malformed head & ataxia	104	29	none	0	none	0
total number phenotypes	262	73	411	29	9	3

Fig. 4. Suppression of *otud3* function interferes with normal anterior development in *Xenopus laevis* embryos. A) Semi-quantitative RT-PCR revealed high maternal expression of *otud3.S* and *otud3.L*. Low levels of *otud3* are maintained during consecutive stages of development following gastrulation (NF 12). To monitor RNA input, *odc1* expression was analyzed. B) Schematic representation of exon-intron structures of *Xenopus laevis otud3* pre-mRNA. Red lines indicate *otud3*-morpholino1 (*otud3*-mo1) and *otud3*-morpholino2 (*otud3*-mo2) target sites. C) Target sequence of *Xenopus laevis otud3* pre-mRNA (black) with corresponding antisense oligonucleotide sequence of *otud3*-mo1 and *otud3*-mo2 (red). The PCR primer and morpholino binding sites are conserved in *otud3.S* and *otud3.L*. D) Injection of *otud3*-mo1/2 at the 2-cell stage led to a strong decrease in *otud3* transcript level in swimming tadpoles (NF stage 36) compared to standard morpholino (std-mo) as shown by semi-quantitative RT-PCR. E) To exclude off-target effects of *otud3*-mo1/2 the level of *p53* expression was compared to mock (std-mo) injected embryos by RT-PCR. F) Injection of *otud3*-mo1/2 led to a pleiotropic phenotype including bent tail, malformed head and eyes, reduced pigmentation, and ataxia (NF stage 38;) compared to mock injected controls. G) Statistical evaluation of morphant phenotypes from three independent experiments (total of 300–400 embryos per experiment). 73 % of *otud3*-mo1/2 injected embryos showed the morphant phenotype at tadpole stage (black). Co-injection with synthetically capped *Xenopus otud3* RNA (*otud3*-mo1/2 + *otud3* RNA; light gray) or synthetically capped human *OTUD3* RNA (*otud3*-mo1/2 + *OTUD3* RNA; gray) clearly demonstrate rescue of the morphant phenotype (by approximately 60 %). Only 3 % of control embryos injected with std-mo (dark gray) developed abnormally. The frequencies of the morphant phenotypes are significant (***, $p < 0.001$; χ^2-test). H) A table summarizes the proportion of *otud3* morphant phenotypes (*otud3*-mo1/2; left) and those rescued by *OTUD3* RNA co-injection (rescue *otud3*; right) compared to mock-injections (std-mo). Commonly observed phenotypes include malformed head associated with ataxia (34 %) or bent tails (29 %). The most severely affected morphants showed both phenotypes (10 %) which was not observed under rescue conditions. (For interpretation of the references to color in this figure legend, the reader is referred to the web version of this article.)

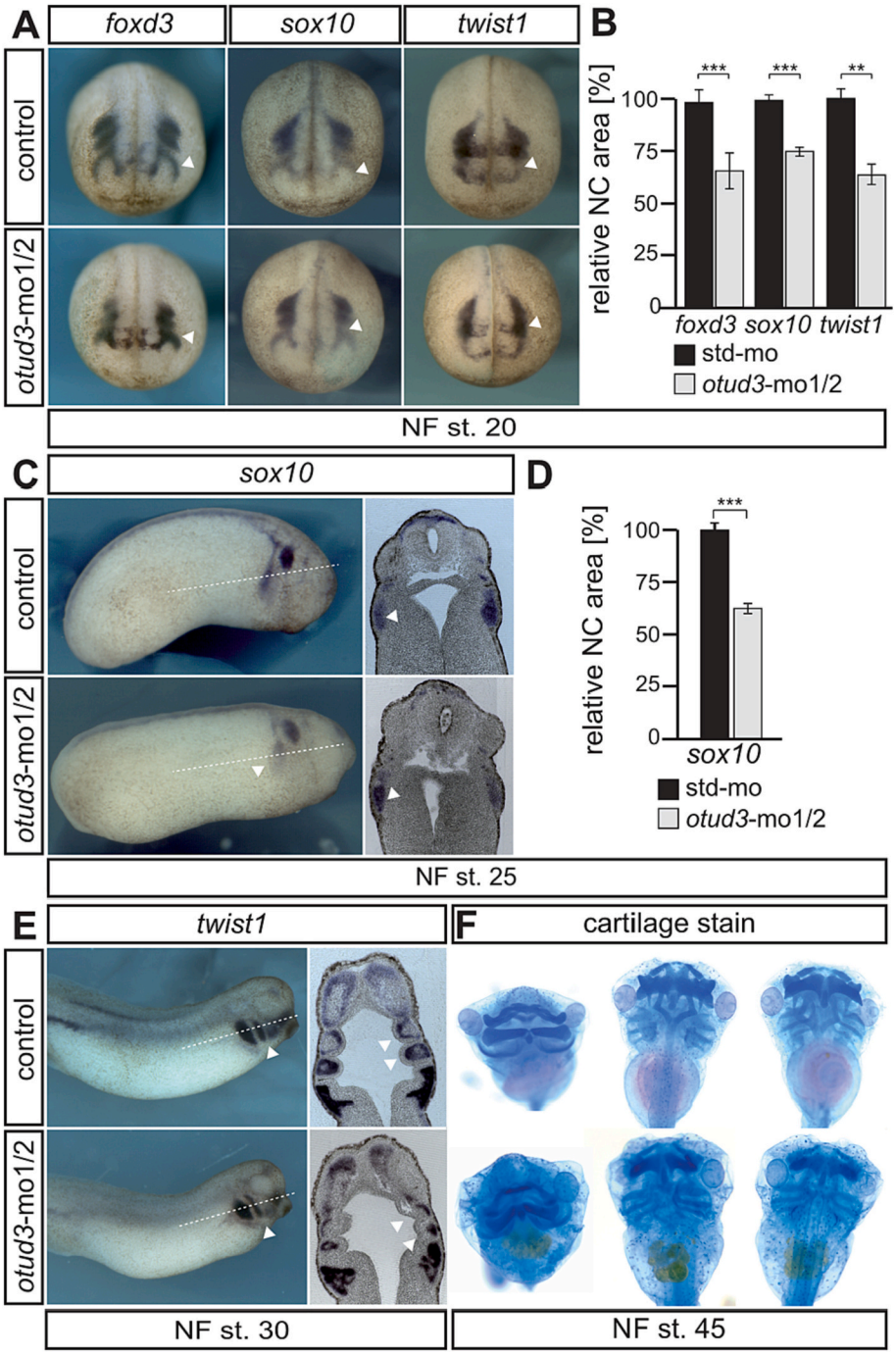

Fig. 5. OTUD3 function is required for proper cranial neural crest specification. A) Whole-mount in situ hybridization (Wmish) of control embryos and *otud3* morphants at NF stage 20. Expression of neural crest (NC) specification genes: *foxd3*, *sox10*, and *twist1* were followed in cranial neural crest cells (NCCs) of NF stage 20 embryos. Loss of *otud3* function led to smaller areas of *foxd3*, *twist1*, and *sox10* expression. Quantification of *foxd3*, *sox10*, and *twist1* expression in cranial neural crest was carried out with ImageJ. Stained NC areas of control embryos as shown in were measured and set to 100 % (std-mo, black). Compared to controls, he areas of expression in *otud3* morphants (*otud3*-mo1/2, gray) are significantly reduced for all marker genes analyzed (**p < 0.01, ***p < 0.001; Student's *t*-test; $N = 8–11$). B) Using *sox10* to mark the hyoid and branchial neural crest cell streams in young tadpoles (NF stage 25) which appear altered in *otud3* morphants compared to controls. White dotted lines indicate the plane of the sections. White triangles indicate neural crest cells. Quantification of relative *sox10* RNA expression detected by Wmish at NF stage 25. Relative NC areas were measured using the ImageJ software. Control embryos (std-mo, black) are normalized to 100 %. In *otud3* morphants (otud3-mo1/2, gray) *sox10* expression is strongly suppressed. Frequencies are highly significant (**p < 0.01, ***p < 0.001; Student's t-test; $N = 9–10$). C) Wmish of control embryos and *otud3* morphants at late tailbud stage (NF stage 30). White dotted lines indicate the plane of sections. NCCs migrating into the mandibular, hyoid, and anterior and posterior branchial streams were marked by *twist1*. *otud3* morphants exhibit shortened branchial and mandibular streams and the hyoid stream is markedly reduced. D) Analysis of the formation of head cartilage by alcian blue cartilage staining in swimming tadpoles. At NF stage 45, Meckels cartilage (ME), ceratohyal cartilage (CE), branchial cartilage (BR), and basihyal cartilage (BA) developed normally in control embryos. *otud3* morphants exhibit compressed and shorted heads with deeper embedded eyes and an edematous body. (For interpretation of the references to color in this figure legend, the reader is referred to the web version of this article.)

throughout all later stages of development (Fig. 4A). To suppress translation of *otud3*, we injected a mixture of two antisense oligonucleotides (morpholino, *otud3*-mo1/2) that block two splice sites of *otud3* pre-mRNA (Fig. 4B, C). Microinjection of *otud3*-mo1/2 morpholinos, but not of control morpholinos, at the two-cell stage led to a strong decrease in *otud3* transcript levels as monitored by sqRT-PCR analysis (Fig. 4D).

We excluded off-target effects of the injected morpholinos as the level of *p53* expression was unaffected by the mock and *otud3* morpholino-injections (Fig. 4E) [66]. Most *otud3* morphants (73 %) developed a spectrum of phenotypic alterations including bent tails, malformed heads and eyes, reduced pigmentation, and a movement disorder (Fig. 4F–H and Supplementary Videos V1 and V2). The specificity of *otud3*-mo1/2 was further examined by injecting *otud3*-mo1/2 together with synthetic *otud3* RNA without morpholino binding sites. In the presence of rescuing RNA, the *otud3* knockdown phenotype was largely reversed. Human synthetic *OTUD3* RNA also rescued the *otud3* morphant phenotype, underlining the high degree of conservation between human OTUD3 and *Xenopus* Otud3 (Fig. 1). Together, these results illustrate that OTUD3 activity is necessary for normal axis formation during development.

3.5. *Otud3 deficiency impairs neural crest development in Xenopus laevis*

Xenopus otud3 morphants showed impaired development of structures derived from neural crest cells, we focused our subsequent analyses on brain and cranial bone formation. Neural crest cells (NCC) can differentiate into numerous derivatives such as melanocytes, cartilage, bone, as well as neurons and glia of the peripheral nervous system [67].

Expression of neural crest-specifier genes (*foxd3*, *sox10* and *twist1*) was slightly reduced in *otud3* morphants as demonstrated by in situ hybridization. This observation was confirmed by sqRT-PCR analysis which showed reduced transcript levels of *foxd3*, *sox10*, and *twist1* in *otud3* morphants compared to mock-injected control embryos (Fig. 5A). In early tadpole-stage embryos (NF stage 25), *sox10* was strongly expressed within the hyoid and branchial streams (Fig. 5B). Migration of NCC upon suppression of *otud3* function was altered in that the hyoid stream was missing and the branchial stream appeared shorter. *twist1* expression indicated a defect in NCC migration at a later NF stage 30, namely NCC migrating into the mandibular, hyoid, and anterior and posterior branchial streams. Here, *otud3* morphants exhibited shortened anterior and posterior branchial streams as well as a smaller mandibular stream, while the hyoid stream was almost lost (Fig. 5C–D). Since these streams of NCC significantly contribute to the cartilaginous anlagen of the head, we performed alcian blue staining of swimming tadpoles at NF stage 45 to follow the development of the craniofacial skeleton. While *otud3* morphants still formed Meckel's (ME), ceratohyal (CE), branchial (BR), and basihyal (BA) cartilages, the presumptive craniofacial skeleton appeared more compact and the development of ME as well as CE was affected (Fig. 5E–F). Taken together, our findings suggest that *otud3* is an important factor not only during the specification of the neural crest cell lineage but also for head and eye development (Supplementary Fig. 3).

4. Discussion

In this study, we investigated the biochemical and molecular properties of the deubiquitinase OTUD3. We found evidence that OTUD3 predominantly localizes in the cytoplasmic space and to a lesser extent in the nucleus. Interestingly, OTUD3 binds to microtubules in the cytoplasm. Thus, nuclear entry may depend on, and thus be regulated by, the interaction between OTUD3 and the dynamics of the microtubular network. We were able to characterize OTUD3 as a deubiquitinase that predominantly cleaves Lys6 and Lys63 linkages and to a much lesser extent Lys11 and Lys 48. Since *OTUD3* transcripts were found to be strongly expressed in RNA preparations of fetal and adult human brains, we investigated the effects of Otud3 suppression of function on the early neural development in *Xenopus* larvae, where it led to impairments in the development of neural crest derivatives like head structures, including the visual system and melanocytes.

The most characteristic features of OTUD3 are the OTU and ubiquitin-associated (UBA) domains which are highly conserved in the chordate phylum ranging from cephalochordates (amphioxus) to humans. The OTU domain forms the proteolytic center with conserved cysteine, aspartate, and histidine as catalytic residues. The UBA domain is often found in proteins involved in ubiquitin-mediated proteolysis with which they can bind polyubiquitin with high affinity. Phylogenetic analysis revealed that mammals and oviparous species form closely related branches. Interestingly, OTUD3 was also identified in sea urchins and oysters, based on a strictly conserved isoleucine of unknown function at the C-terminal end. To our knowledge, lipoxygenases are the only other class of proteins in which a C-terminal isoleucine is conserved. Here, the isoleucine is likely critical for the formation of a C-terminal helix that is important for iron binding and oxidative enzyme activity [68–70]. It is still unknown whether OTUD3 or any other member of the OTU family forms a helix-like domain at the C-terminus or whether it is a metal-binding protein.

Using tetra-ubiquitin chains of defined linkages we found that OTUD3 can cleave Lys11 and Lys48 linked polyubiquitin with low activity (Fig. 3). Both forms have been implicated in targeting substrate proteins to the proteasome for degradation. While Lys11 and Lys48 appear equally abundant in cells, much less is known about the function of Lys11-linked compared to K48-linked polyubiquitin, the latter being known as classical signal for protein degradation [71–73]. Interestingly, OTUD7A and OTUD7B (Cezanne-2 and Cezanne) are the only deubiquitinases described so far to cleave Lys11-polyubiquitin chains, pointing toward the existence of a regulated degradation pathway independent of Lys48 and with potentially important roles in Parkinson's disease, DNA-damage response, and hypoxia regulation [47,52,71,74–76]. Even branched polyubiquitin chains via Lys11 and Lys48 had been described that enhance protein degradation by increasing the affinity for the proteasome [77,78].

We found OTUD3 to be highly efficient in cleaving Lys6 and Lys63 polyubiquitin (Fig. 3). Cleavage of Lys63-linked polyubiquitin by OTUD3 has been reported recently [79]. BRCA1/BARD1 heterodimers form an E3-ligase that directs the formation of Lys6 linkages, probably helped by UBXN1, which play a role in DNA repair, DNA replication, and transcriptional regulation. In the BRCA-mediated DNA repair pathway, Lys6-modified ubiquitin chains possess a regulatory rather than degradation function [80–84]. Moreover, it has been reported recently that Lys6-linked ubiquitin chains can induce the degradation of a tyrosine phosphatase in the nucleus [85]. A minor fraction of OTUD3 localizes to the nucleus of unstressed cells (Fig. 2). Although the exact role of nuclear OTUD3 remains to be investigated, the idea that OTUD3 might be involved in silencing (e.g., through DNA-repair) pathways by counteracting Lys6 ubiquitination when not required is intriguing.

E3-ligase Parkin and USP30 can respectively assemble and disassemble Lys6-linked polyubiquitin. Parkin ubiquitinates damage mitochondria for their degradation. USP30, like USP8 deubiquitinase, opposes Parkin activity on mitochondria since they preferentially cleave Lys6-linked polyubiquitin. Recently, *Otud3* has been described to prevent Parkinson's disease in a mouse model [86–89]. In addition, Lys63-linked ubiquitin chains have been associated with neuronal dysfunction like ataxia, autism-like behaviors, proper function in neuronal excitatory postsynapses [90–92]. *Otud3*-morphants displayed an ataxia-like phenotype with seizures at tadpole stage and the tadpole's movement appeared undirected (Supplementary Videos 1 and 2). A similar phenotype was observed in *trim2*-morphants and in *Trim2*-knockout mice but also *Otud3*-knockout mice. TRIM2 is a E3-ligase which physically interacts with ALIX (ALG-2 interacting protein X), a Lys63-specific polyubiquitin binding protein that can block apoptosis and functions during endocytosis. While no ubiquitin linkage type has been attributed to Trim2, Lys63-ubiquitin chains are involved in a variety of vesicle trafficking events and protein sorting [89,93–98]. Surprisingly, free K63-linked polyubiquitin chains bind to DNA and enhance the recruitment of repair factors to damaged DNA [99,100]. Whether OTUD3 is involved in the resolution of Lys63 polyubiquitin containing repair complexes has not been invested. In this context, it is interesting to note that during DNA damage the Mahogunin Ring Finger-1 (MGRN1) containing ubiquitin ligase mediates the Lys6 ubiquitination of alpha-tubulin to regulate microtubule stability and mitotic spindle orientation [81,101]. We found that OTUD3 can bind to microtubules and is able to cleave Lys6 polyubiquitin chains with high efficiency. It will be interesting to test whether OTUD3 antagonizes MGRN1 in this process. In fact, many microtubules associated DUBs like USP9X, USP35, USP44, AMSH, CYLD or CEZANNE, are expressed in a cell-cycle dependent manner or change their location concomitantly [77]. As an example, CYLD localizes to microtubules during interphase, migrates to the midbody during telophase and CYLD protein levels decrease after mitosis. Depletion of CYLD resulted in delayed mitosis entry, whereas overexpression coincided with fragmented or multinucleated cells, impaired chromosome segregation and cytokinesis [102,103]. Several reported substrates of OTUD3 including ACTN4 [30], p53 [104], and PTEN [105] are present in the cytosol and in the nucleus. Among them, the tumor suppressor p53 is even associated with cellular microtubules and translocates to the nucleus in a dynein dependent manner [106]. Near the nucleus, p53 is translocated into the nucleus with the help of importin-α3 and heat shock factor Hsf1 [107,108]. In our experiments, OTUD3 is mostly present in the cytosol and co-localizes with microtubules, with a minor signal in the nucleus. It is thus possible that similar to p53, OTUD3 binds to microtubules to allow directional transport

toward the periphery of the nucleus for efficient nuclear translocation. In another hypothetic scenario, OTUD3 functions as a DUB that deubiquitylates tubulin or tubulin-associated proteins. It is of note that cleavage of Lys6 and Lys63 polyubiquitin chains has also been reported to regulate innate immunity upon pathogen infection [109]. Taken together, OTUD could probably be involved in shutting down stress responses like DNA damage and infections counteracting Lys6 and Lys63 dependent signaling.

Through loss-of-function experiments we showed that OTUD3/Otud3 is essential for normal early embryonic development. Neurocranial structures and neural crest specification were strongly affected in *otud3*-morphants. The most notable effects were loss of pigmentation and formation of smaller heads with dysplasia of the presumptive head skeleton. Both tissues descend - at least partially - from the neural crest. Interestingly, in dark-furred mahoganoid mice the above-mentioned Mgrn1 E3-ligase is absent and Mgrn1-null melanocytes are hyperpigmented. Thus, loss-of-function of Otud3 and of TRIM2 show corresponding phenotypes in neural crest derived cells [110]. The neural crest cells arise in regions with intermediate levels of BMP, between the neural- and non-neural ectoderm. High levels of BMP induce formation of epidermis and low levels of BMP promote neural ectodermal differentiation [111,112]. Malformation of neural crest derivatives may result from a spatial shift or a steeper gradient of BMP expression, with higher BMP activity in the region of the developing neural plate. Regular head formation in amphibian embryos requires the suppression of WNT and BMP signals emanating from ectoderm and ventral mesoderm [113]. Thus, the small head of *otud3* morphants may reflect higher regional BMP signaling. Accordingly, the formation of neural structures was also impaired upon suppression of *otud3* function and a mild repression of BMP-signaling was observed in pluripotent animal cap cells (*Xenopus* animal cap assay) upon *otud3*-knockdown (Supplementary Fig. 3). Ubiquitination regulates several vital proteins involved in BMP-signaling. BMPR-IA is triggered for degradation by UBE3A [114]. NIPA1 interacts with BMPR2 and promotes its endocytosis and lysosomal degradation [115,116]. Smurf1 E3 ubiquitin ligase is involved in endocytosis/recycling and lysosomal degradation of BMPR [117,118]. In contrast, USP15 and OTUD4 protect BMPR1A as well as SMAD4 from degradation [119–122]. Thus, OTUD3 is likely part of this complex network regulating BMP signaling activity during early development, probably at the level of vesicle trafficking, which is strongly related to Lys63 ubiquitin signaling.

Overall, we conclude that OTUD3 function is required for early specification of the neural crest linage and most likely for proper BMP signaling in *Xenopus* embryos. Moreover, we could characterize OTUD3 as a deubiquitinase that can bind to microtubules and predominantly cleaves Lys6 and Lys63 linkages and, to a lesser extent, Lys11 and Lys 48, which suggests its involvement primarily in converting protein activity rather than in protein degradation.

Supplementary data to this article can be found online at https://doi.org/10.1016/j.bbagrm.2022.194901.

Funding

The project was supported by Roux 28/44 (MLU, Medical Faculty Halle-Wittenberg) and Deutsche Forschungsgemeinschaft (DFG) HO2597/2-1.

CRediT authorship contribution statement

CM performed the embryonic work on *Xenopus*; FJ & TP performed qPCR and immunofluorescence; TP provided advice on how to perform enzyme tests; JH & HN performed in situ hybridization and histology and performed catalytic analysis of OTUD3; KH & PL contributed to the research design. TH was the major contributor to manuscript writing and preparation, all authors have read and approved the final manuscript.

Declaration of competing interest

The authors declare that they have no known competing financial interests or personal relationships that could have appeared to influence the work reported in this paper.

Data availability

Data will be made available on request.

Acknowledgments

We thank David Komander and Kristin Henningfeld for plasmids.

References

[1] A. Hershko, A. Ciechanover, The ubiquitin system, Annu. Rev. Biochem. 67 (1998) 425–479.
[2] L. Hicke, R. Dunn, Regulation of membrane protein transport by ubiquitin and ubiquitin-binding proteins, Annu. Rev. Cell Dev. Biol. 19 (2003) 141–172.
[3] C.M. Pickart, Back to the future with ubiquitin, Cell 116 (2004) 181–190.
[4] B.T. Dye, B.A. Schulman, Structural mechanisms underlying posttranslational modification by ubiquitin-like proteins, Annu. Rev. Biophys. Biomol. Struct. 36 (2007) 131–150.
[5] D. Komander, The emerging complexity of protein ubiquitination, Biochem. Soc. Trans. 37 (2009) 937–953.
[6] C.H. Emmerich, A. Ordureau, S. Strickson, J.S. Arthur, P.G. Pedrioli, D. Komander, P. Cohen, Activation of the canonical IKK complex by K63/M1-linked hybrid ubiquitin chains, Proc. Natl. Acad. Sci. U. S. A. 110 (2013) 15247–15252.
[7] W. Kim, E.J. Bennett, E.L. Huttlin, A. Guo, J. Li, A. Possemato, M.E. Sowa, R. Rad, J. Rush, M.J. Comb, J.W. Harper, S.P. Gygi, Systematic and quantitative assessment of the ubiquitin-modified proteome, Mol. Cell 44 (2011) 325–340.
[8] A.Y. Amerik, M. Hochstrasser, Mechanism and function of deubiquitinating enzymes, Biochim. Biophys. Acta 1695 (2004) 189–207.
[9] S.M. Nijman, M.P. Luna-Vargas, A. Velds, T.R. Brummelkamp, A.M. Dirac, T. K. Sixma, R. Bernards, A genomic and functional inventory of deubiquitinating enzymes, Cell 123 (2005) 773–786.
[10] F.E. Reyes-Turcu, K.H. Ventii, K.D. Wilkinson, Regulation and cellular roles of ubiquitin-specific deubiquitinating enzymes, Annu. Rev. Biochem. 78 (2009) 363–397.
[11] A.C. Faesen, M.P. Luna-Vargas, P.P. Geurink, M. Clerici, R. Merkx, W.J. van Dijk, D.S. Hameed, F. El Oualid, H. Ovaa, T.K. Sixma, The differential modulation of USP activity by internal regulatory domains, interactors and eight ubiquitin chain types, Chem. Biol. 18 (2011) 1550–1561.
[12] T.E. Mevissen, M.K. Hospenthal, P.P. Geurink, P.R. Elliott, M. Akutsu, N. Arnaudo, R. Ekkebus, Y. Kulathu, T. Wauer, F. El Oualid, S.M. Freund, H. Ovaa, D. Komander, OTU deubiquitinases reveal mechanisms of linkage specificity and enable ubiquitin chain restriction analysis, Cell 154 (2013) 169–184.
[13] I.E. Wertz, K.M. O'Rourke, H. Zhou, M. Eby, L. Aravind, S. Seshagiri, P. Wu, C. Wiesmann, R. Baker, D.L. Boone, A. Ma, E.V. Koonin, V.M. Dixit, De-ubiquitination and ubiquitin ligase domains of A20 downregulate NF-kappaB signalling, Nature 430 (2004) 694–699.
[14] M. Akutsu, I. Dikic, A. Bremm, Ubiquitin chain diversity at a glance, J. Cell Sci. 129 (2016) 875–880.
[15] M.J. Clague, S. Urbe, D. Komander, Breaking the chains: deubiquitylating enzyme specificity begets function, Nat. Rev. Mol. Cell Biol. 20 (2019) 338–352.
[16] P.R. Elliott, D. Leske, J. Wagstaff, L. Schlicher, G. Berridge, S. Maslen, F. Timmermann, B. Ma, R. Fischer, S.M.V. Freund, D. Komander, M. Gyrd-Hansen, Regulation of CYLD activity and specificity by phosphorylation and ubiquitin-binding CAP-Gly domains, Cell Rep. 37 (2021), 109777.
[17] L. Herhaus, I. Dikic, Expanding the ubiquitin code through post-translational modification, EMBO Rep. 16 (2015) 1071–1083.
[18] S. Piao, H.Z. Pei, B. Huang, S.H. Baek, Ovarian tumor domain-containing protein 1 deubiquitinates and stabilizes p53, Cell. Signal. 33 (2017) 22–29.
[19] Z. Zhang, D. Wang, P. Wang, Y. Zhao, F. You, OTUD1 negatively regulates type I IFN induction by disrupting noncanonical ubiquitination of IRF3, J. Immunol. 204 (2020) 1904–1918.
[20] F. Yao, Z. Xiao, Y. Sun, L. Ma, SKP2 and OTUD1 govern non-proteolytic ubiquitination of YAP that promotes YAP nuclear localization and activity, CellStress 2 (2018) 233–235.
[21] W. Liu, B. Yan, H. Yu, J. Ren, M. Peng, L. Zhu, Y. Wang, X. Jin, L. Yi, OTUD1 stabilizes PTEN to inhibit the PI3K/AKT and TNF-alpha/NF-kappaB signaling pathways and sensitize ccRCC to TKIs, Int. J. Biol. Sci. 18 (2022) 1401–1414.
[22] G. Schimmack, K. Schorpp, K. Kutzner, T. Gehring, J.K. Brenke, K. Hadian, D. Krappmann, YOD1/TRAF6 association balances p62-dependent IL-1 signaling to NF-kappaB, elife 6 (2017).
[23] J.H. Park, S.Y. Kim, H.J. Cho, S.Y. Lee, K.H. Baek, YOD1 deubiquitinates NEDD4 involved in the Hippo signaling pathway, Cell. Physiol. Biochem. 54 (2020) 1–14.

[24] L. Yuan, Y. Lv, H. Li, H. Gao, S. Song, Y. Zhang, G. Xing, X. Kong, L. Wang, Y. Li, T. Zhou, D. Gao, Z.X. Xiao, Y. Yin, W. Wei, F. He, L. Zhang, Deubiquitylase OTUD3 regulates PTEN stability and suppresses tumorigenesis, Nat. Cell Biol. 17 (2015) 1169–1181.

[25] Y. Zhao, M.C. Mudge, J.M. Soll, R.B. Rodrigues, A.K. Byrum, E.A. Schwarzkopf, T. R. Bradstreet, S.P. Gygi, B.T. Edelson, N. Mosammaparast, OTUD4 is a phospho-activated K63 deubiquitinase that regulates MyD88-dependent signaling, Mol. Cell 69 (2018) 505–516 e505.

[26] X. Zhao, X. Su, L. Cao, T. Xie, Q. Chen, J. Li, R. Xu, C. Jiang, OTUD4: a potential prognosis biomarker for multiple human cancers, Cancer Manag. Res. 12 (2020) 1503–1512.

[27] T. Du, H. Li, Y. Fan, L. Yuan, X. Guo, Q. Zhu, Y. Yao, X. Li, C. Liu, X. Yu, Z. Liu, C. P. Cui, C. Han, L. Zhang, The deubiquitylase OTUD3 stabilizes GRP78 and promotes lung tumorigenesis, Nat. Commun. 10 (2019) 2914.

[28] Q. Pu, Y.R. Lv, K. Dong, W.W. Geng, H.D. Gao, Tumor suppressor OTUD3 induces growth inhibition and apoptosis by directly deubiquitinating and stabilizing p53 in invasive breast carcinoma cells, BMC Cancer 20 (2020) 583.

[29] P. Zhang, C. Li, H. Li, L. Yuan, H. Dai, Z. Peng, Z. Deng, Z. Chang, C.P. Cui, L. Zhang, Ubiquitin ligase CHIP regulates OTUD3 stability and suppresses tumour metastasis in lung cancer, Cell Death Differ 27 (2020) 3177–3195.

[30] P. Xie, Y. Chen, H. Zhang, G. Zhou, Q. Chao, J. Wang, Y. Liu, J. Fang, J. Xie, J. Zhen, Z. Wang, L. Hao, D. Huang, The deubiquitinase OTUD3 stabilizes ACTN4 to drive growth and metastasis of hepatocellular carcinoma, Aging (Albany NY) 13 (2021) 19317–19338.

[31] X. Cai, Z. Zhou, J. Zhu, X. Liu, G. Ouyang, J. Wang, Z. Li, X. Li, H. Zha, C. Zhu, F. Rong, J. Tang, Q. Liao, X. Chen, W. Xiao, Opposing effects of deubiquitinase OTUD3 in innate immunity against RNA and DNA viruses, Cell Rep. 39 (2022), 110920.

[32] M. Wang, Y. Li, Y. Xiao, M. Yang, J. Chen, Y. Jian, X. Chen, D. Shi, X. Chen, Y. Ouyang, L. Kong, X. Huang, J. Bai, C. Lin, L. Song, Nicotine-mediated OTUD3 downregulation inhibits VEGF-C mRNA decay to promote lymphatic metastasis of human esophageal cancer, Nat. Commun. 12 (2021) 7006.

[33] D.H. Margolin, M. Kousi, Y.M. Chan, E.T. Lim, J.D. Schmahmann, M. Hadjivassiliou, J.E. Hall, I. Adam, A. Dwyer, L. Plummer, S.V. Aldrin, J. O'Rourke, A. Kirby, K. Lage, A. Milunsky, J.M. Milunsky, J. Chan, E.T. Hedley-Whyte, M.J. Daly, N. Katsanis, S.B. Seminara, Ataxia, dementia, and hypogonadotropism caused by disordered ubiquitination, N. Engl. J. Med. 368 (2013) 1992–2003.

[34] P.W. Jaynes, P.V. Iyengar, S.K.L. Lui, T.Z. Tan, N. Vasilevski, S.C.E. Wright, G. Verdile, A.D. Jeyasekharan, P.J.A. Eichhorn, OTUD4 enhances TGFbeta signalling through regulation of the TGFbeta receptor complex, Sci. Rep. 10 (2020) 15725.

[35] N. Kayagaki, Q. Phung, S. Chan, R. Chaudhari, C. Quan, K.M. O'Rourke, M. Eby, E. Pietras, G. Cheng, J.F. Bazan, Z. Zhang, D. Arnott, V.M. Dixit, DUBA: a deubiquitinase that regulates type I interferon production, Science 318 (2007) 1628–1632.

[36] S. Rutz, N. Kayagaki, Q.T. Phung, C. Eidenschenk, R. Noubade, X. Wang, J. Lesch, R. Lu, K. Newton, O.W. Huang, A.G. Cochran, M. Vasser, B.P. Fauber, J. DeVoss, J. Webster, L. Diehl, Z. Modrusan, D.S. Kirkpatrick, J.R. Lill, W. Ouyang, V. M. Dixit, Deubiquitinase DUBA is a post-translational brake on interleukin-17 production in T cells, Nature 518 (2015) 417–421.

[37] Y. Zhang, Y. Fan, X. Jing, L. Zhao, T. Liu, L. Wang, L. Zhang, S. Gu, X. Zhao, Y. Teng, OTUD5-mediated deubiquitination of YAP in macrophage promotes M2 phenotype polarization and favors triple-negative breast cancer progression, Cancer Lett. 504 (2021) 104–115.

[38] J. Luo, Z. Lu, X. Lu, L. Chen, J. Cao, S. Zhang, Y. Ling, X. Zhou, OTUD5 regulates p53 stability by deubiquitinating p53, PLoS One 8 (2013), e77682.

[39] A. de Vivo, A. Sanchez, J. Yegres, J. Kim, S. Emly, Y. Kee, The OTUD5-UBR5 complex regulates FACT-mediated transcription at damaged chromatin, Nucleic Acids Res. 47 (2019) 729–746.

[40] F. Yin, H. He, B. Zhang, J. Zheng, M. Wang, M. Zhang, H. Cui, Effect of deubiquitinase ovarian tumor domain-containing protein 5 (OTUD5) on radiosensitivity of cervical cancer by regulating the ubiquitination of Akt and its mechanism, Med. Sci. Monit. 25 (2019) 3469–3475.

[41] F. Li, Q. Sun, K. Liu, H. Han, N. Lin, Z. Cheng, Y. Cai, F. Tian, Z. Mao, T. Tong, W. Zhao, The deubiquitinase OTUD5 regulates Ku80 stability and non-homologous end joining, Cell. Mol. Life Sci. 76 (2019) 3861–3873.

[42] T. Santiago-Sim, L.C. Burrage, F. Ebstein, M.J. Tokita, M. Miller, W. Bi, A. A. Braxton, J.A. Rosenfeld, M. Shahrour, A. Lehmann, B. Cogne, S. Kury, T. Besnard, B. Isidor, S. Bezieau, I. Hazart, H. Nagakura, L.L. Immken, R. O. Littlejohn, E. Roeder, , S.H.C. EuroEpinomics Res Consortium Autosomal Recessive working group, B. Kara, K. Hardies, S. Weckhuysen, P. May, J. R. Lemke, O. Elpeleg, B. Abu-Libdeh, K.N. James, J.L. Silhavy, M.Y. Issa, M. S. Zaki, J.G. Gleeson, J.R. Seavitt, M.E. Dickinson, M.C. Ljungberg, S. Wells, S. J. Johnson, L. Teboul, C.M. Eng, Y. Yang, P.M. Kloetzel, J.D. Heaney, M. A. Walkiewicz, Biallelic variants in OTUD6B cause an intellectual disability syndrome associated with seizures and dysmorphic features, Am. J. Hum. Genet. 100 (2017) 676–688.

[43] G.M.H. Abdel-Salam, M.S. Abdel-Hamid, I.S.M. Sayed, U. Zechner, H.J. Bolz, OTUD6B-associated intellectual disability: novel variants and genetic exclusion of retinal degeneration as part of a refined phenotype, J. Hum. Genet. 67 (2022) 55–64.

[44] A. Sobol, C. Askonas, S. Alani, M.J. Weber, V. Ananthanarayanan, C. Osipo, M. Bocchetta, Deubiquitinase OTUD6B isoforms are important regulators of growth and proliferation, Mol. Cancer Res. 15 (2017) 117–127.

[45] K. Enesa, M. Zakkar, H. Chaudhury, A. Luong le, L. Rawlinson, J.C. Mason, D. O. Haskard, J.L. Dean, P.C. Evans, NF-kappaB suppression by the deubiquitinating enzyme Cezanne: a novel negative feedback loop in pro-inflammatory signaling, J. Biol. Chem. 283 (2008) 7036–7045.

[46] A. Bremm, D. Komander, Emerging roles for Lys11-linked polyubiquitin in cellular regulation, Trends Biochem 36 (2011) 355–363.

[47] T.E.T. Mevissen, Y. Kulathu, M.P.C. Mulder, P.P. Geurink, S.L. Maslen, M. Gersch, P.R. Elliott, J.E. Burke, B.D.M. van Tol, M. Akutsu, F.E. Oualid, M. Kawasaki, S.M. V. Freund, H. Ovaa, D. Komander, Molecular basis of Lys11-polyubiquitin specificity in the deubiquitinase Cezanne, Nature 538 (2016) 402–405.

[48] Z. Xu, L. Pei, L. Wang, F. Zhang, X. Hu, Y. Gui, Snail1-dependent transcriptional repression of Cezanne2 in hepatocellular carcinoma, Oncogene 33 (2014) 2836–2845.

[49] M. Uddin, B.K. Unda, V. Kwan, N.T. Holzapfel, S.H. White, L. Chalil, M. Woodbury-Smith, K.S. Ho, E. Harward, N. Murtaza, B. Dave, G. Pellecchia, L. D'Abate, T. Nalpathamkalam, S. Lamoureux, J. Wei, M. Speevak, J. Stavropoulos, K.J. Hope, B.W. Doble, J. Nielsen, E.R. Wassman, S.W. Scherer, K.K. Singh, OTUD7A regulates neurodevelopmental phenotypes in the 15q13.3 microdeletion syndrome, Am. J. Hum. Genet. 102 (2018) 278–295.

[50] J. Yin, W. Chen, E.S. Chao, S. Soriano, L. Wang, W. Wang, S.E. Cummock, H. Tao, K. Pang, Z. Liu, F.A. Pereira, R.C. Samaco, H.Y. Zoghbi, M. Xue, C.P. Schaaf, Otud7a knockout mice recapitulate many neurological features of 15q13.3 microdeletion syndrome, Am. J. Hum. Genet. 102 (2018) 296–308.

[51] H. Suzuki, M. Inaba, M. Yamada, T. Uehara, T. Takenouchi, S. Mizuno, K. Kosaki, M. Doi, Biallelic loss of OTUD7A causes severe muscular hypotonia, intellectual disability, and seizures, Am. J. Med. Genet. A 185 (2021) 1182–1186.

[52] A. Bremm, S. Moniz, J. Mader, S. Rocha, D. Komander, Cezanne (OTUD7B) regulates HIF-1alpha homeostasis in a proteasome-independent manner, EMBO Rep. 15 (2014) 1268–1277.

[53] A. Luong le, M. Fragiadaki, J. Smith, J. Boyle, J. Lutz, J.L. Dean, S. Harten, M. Ashcroft, S.R. Walmsley, D.O. Haskard, P.H. Maxwell, H. Walczak, C. Pusey, P. C. Evans, Cezanne regulates inflammatory responses to hypoxia in endothelial cells by targeting TRAF6 for deubiquitination, Circ. Res. 112 (2013) 1583–1591.

[54] S. Moniz, D. Bandarra, J. Biddlestone, K.J. Campbell, D. Komander, A. Bremm, S. Rocha, Cezanne regulates E2F1-dependent HIF2alpha expression, J. Cell Sci. 128 (2015) 3082–3093.

[55] W. Xie, S. Tian, J. Yang, S. Cai, S. Jin, T. Zhou, Y. Wu, Z. Chen, Y. Ji, J. Cui, OTUD7B deubiquitinates SQSTM1/p62 and promotes IRF3 degradation to regulate antiviral immunity, Autophagy (2022) 1–15.

[56] A. Lokapally, S. Metikala, T. Hollemann, Xenopus laevis neuronal cell adhesion molecule (nrcam): plasticity of a CAM in the developing nervous system, Dev. Genes Evol. 227 (2017) 61–67.

[57] K.J. Livak, T.D. Schmittgen, Analysis of relative gene expression data using real-time quantitative PCR and the 2(-Delta Delta C(T)) method, Methods 25 (2001) 402–408.

[58] T. Hollemann, E. Tadjuidje, K. Koebernick, T. Pieler, Manipulation of hedgehog signaling in Xenopus by means of embryo microinjection and application of chemical inhibitors, Methods Mol. Biol. 397 (2007) 35–45.

[59] P.D. Nieuwkoop, J. Faber, Normal Table of Xenopus laevis (Daudin), North Holland, Amsterdam, 1967.

[60] T. Pfirrmann, A. Lokapally, C. Andreasson, P. Ljungdahl, T. Hollemann, SOMA: a single oligonucleotide mutagenesis and cloning approach, PLoS One 8 (2013), e64870.

[61] T. Hollemann, Y. Chen, H. Grunz, T. Pieler, Regionalized metabolic activity establishes boundaries of retinoic acid signalling, EMBO J. 17 (1998) 7361–7372.

[62] S. Gessert, D. Maurus, A. Rossner, M. Kuhl, Pescadillo is required for Xenopus laevis eye development and neural crest migration, Dev. Biol. 310 (2007) 99–112.

[63] M.Y. Balakirev, S.O. Tcherniuk, M. Jaquinod, J. Chroboczek, Otubains: a new family of cysteine proteases in the ubiquitin pathway, EMBO Rep. 4 (2003) 517–522.

[64] K.S. Makarova, L. Aravind, E.V. Koonin, A novel superfamily of predicted cysteine proteases from eukaryotes, viruses and Chlamydia pneumoniae, Trends Biochem. Sci. 25 (2000) 50–52.

[65] M.E. Morrow, M.T. Morgan, M. Clerici, K. Growkova, M. Yan, D. Komander, T. K. Sixma, M. Simicek, C. Wolberger, Active site alanine mutations convert deubiquitinases into high-affinity ubiquitin-binding proteins, EMBO Rep. 19 (2018).

[66] M.E. Robu, J.D. Larson, A. Nasevicius, S. Beiraghi, C. Brenner, S.A. Farber, S. C. Ekker, p53 activation by knockdown technologies, PLoS Genet. 3 (2007), e78.

[67] S.A. Green, M. Simoes-Costa, M.E. Bronner, Evolution of vertebrates as viewed from the crest, Nature 520 (2015) 474–482.

[68] X.S. Chen, C.D. Funk, The N-terminal "beta-barrel" domain of 5-lipoxygenase is essential for nuclear membrane translocation, J. Biol. Chem. 276 (2001) 811–818.

[69] T. Hammarberg, Y.Y. Zhang, B. Lind, O. Radmark, B. Samuelsson, Mutations at the C-terminal isoleucine and other potential iron ligands of 5-lipoxygenase, Eur. J. Biochem. 230 (1995) 401–407.

[70] N.C. Gilbert, S.G. Bartlett, M.T. Waight, D.B. Neau, W.E. Boeglin, A.R. Brash, M. E. Newcomer, The structure of human 5-lipoxygenase, Science 331 (2011) 217–219.

[71] A. Bremm, S.M. Freund, D. Komander, Lys11-linked ubiquitin chains adopt compact conformations and are preferentially hydrolyzed by the deubiquitinase Cezanne, Nat. Struct. Mol. Biol. 17 (2010) 939–947.

[72] V. Chau, J.W. Tobias, A. Bachmair, D. Marriott, D.J. Ecker, D.K. Gonda, A. Varshavsky, A multiubiquitin chain is confined to specific lysine in a targeted short-lived protein, Science 243 (1989) 1576–1583.

[73] J.S. Thrower, L. Hoffman, M. Rechsteiner, C.M. Pickart, Recognition of the polyubiquitin proteolytic signal, EMBO J. 19 (2000) 94–102.
[74] X. Wu, S. Liu, C. Sagum, J. Chen, R. Singh, A. Chaturvedi, J.R. Horton, T. R. Kashyap, D. Fushman, X. Cheng, M.T. Bedford, B. Wang, Crosstalk between Lys63- and Lys11-polyubiquitin signaling at DNA damage sites is driven by cezanne, Genes Dev. 33 (2019) 1702–1717.
[75] M. Locke, J.I. Toth, M.D. Petroski, Lys11- and Lys48-linked ubiquitin chains interact with p97 during endoplasmic-reticulum-associated degradation, Biochem. J. 459 (2014) 205–216.
[76] K.K. Deol, S.J. Eyles, E.R. Strieter, Quantitative middle-down MS analysis of parkin-mediated ubiquitin chain assembly, J. Am. Soc. Mass Spectrom. 31 (2020) 1132–1139.
[77] A.J. Boughton, S. Krueger, D. Fushman, Branching via K11 and K48 bestows ubiquitin chains with a unique interdomain interface and enhanced affinity for proteasomal subunit Rpn1, Structure 28 (2020) 29–43 e26.
[78] H.J. Meyer, M. Rape, Enhanced protein degradation by branched ubiquitin chains, Cell 157 (2014) 910–921.
[79] Z. Zhang, X. Fang, X. Wu, L. Ling, F. Chu, J. Li, S. Wang, J. Zang, B. Zhang, S. Ye, L. Zhang, B. Yang, S. Lin, H. Huang, A. Wang, F. Zhou, Acetylation-dependent deubiquitinase OTUD3 controls MAVS activation in innate antiviral immunity, Mol. Cell 79 (2020) 304–319, e307.
[80] S.R. Witus, M.D. Stewart, R.E. Klevit, The BRCA1/BARD1 ubiquitin ligase and its substrates, Biochem. J. 478 (2021) 3467–3483.
[81] F. Wu-Baer, K. Lagrazon, W. Yuan, R. Baer, The BRCA1/BARD1 heterodimer assembles polyubiquitin chains through an unconventional linkage involving lysine residue K6 of ubiquitin, J. Biol. Chem. 278 (2003) 34743–34746.
[82] J.R. Morris, E. Solomon, BRCA1: BARD1 induces the formation of conjugated ubiquitin structures, dependent on K6 of ubiquitin, in cells during DNA replication and repair, Hum. Mol. Genet. 13 (2004) 807–817.
[83] F. Shang, G. Deng, Q. Liu, W. Guo, A.L. Haas, B. Crosas, D. Finley, A. Taylor, Lys6-modified ubiquitin inhibits ubiquitin-dependent protein degradation, J. Biol. Chem. 280 (2005) 20365–20374.
[84] D. Shahul Hameed, G.B.A. van Tilburg, R. Merkx, D. Flierman, H. Wienk, F. El Oualid, K. Hofmann, R. Boelens, H. Ovaa, Diubiquitin-based NMR analysis: interactions between Lys6-linked diUb and UBA domain of UBXN1, Front. Chem. 7 (2019) 921.
[85] Q. Wang, C. Xu, R. Cai, W. An, H. Yuan, M. Xu, Fbxo45-mediated NP-STEP46 degradation via K6-linked ubiquitination sustains ERK activity in lung cancer, Mol. Oncol. 16 (2022) 3017–3033.
[86] T.M. Durcan, M.Y. Tang, J.R. Perusse, E.A. Dashti, M.A. Aguileta, G.L. McLelland, P. Gros, T.A. Shaler, D. Faubert, B. Coulombe, E.A. Fon, USP8 regulates mitophagy by removing K6-linked ubiquitin conjugates from parkin, EMBO J. 33 (2014) 2473–2491.
[87] M. Gersch, C. Gladkova, A.F. Schubert, M.A. Michel, S. Maslen, D. Komander, Mechanism and regulation of the Lys6-selective deubiquitinase USP30, Nat. Struct. Mol. Biol. 24 (2017) 920–930.
[88] Y. Sato, K. Okatsu, Y. Saeki, K. Yamano, N. Matsuda, A. Kaiho, A. Yamagata, S. Goto-Ito, M. Ishikawa, Y. Hashimoto, K. Tanaka, S. Fukai, Structural basis for specific cleavage of Lys6-linked polyubiquitin chains by USP30, Nat. Struct. Mol. Biol. 24 (2017) 911–919.
[89] F. Jia, H. Li, Q. Jiao, C. Li, L. Fu, C. Cui, H. Jiang, L. Zhang, Deubiquitylase OTUD3 prevents Parkinson's disease through stabilizing iron regulatory protein 2, Cell Death Dis. 13 (2022) 418.
[90] E. Colombo, G. Horta, M.K. Roesler, N. Ihbe, S. Chhabra, K. Radyushkin, G. Di Liberto, M. Kreutzfeldt, S. Schumann, J. von Engelhardt, D. Merkler, C. Behl, T. Mittmann, A.M. Clement, A. Waisman, M.J. Schmeisser, The K63 deubiquitinase CYLD modulates autism-like behaviors and hippocampal plasticity by regulating autophagy and mTOR signaling, Proc. Natl. Acad. Sci. U. S. A. 118 (2021).
[91] S. Kim, Y. Zhang, C. Jin, Y. Lee, Y. Kim, K. Han, Emerging roles of Lys63-linked polyubiquitination in neuronal excitatory postsynapses, Arch. Pharm. Res. 42 (2019) 285–292.
[92] Y. Sato, E. Goto, Y. Shibata, Y. Kubota, A. Yamagata, S. Goto-Ito, K. Kubota, J. Inoue, M. Takekawa, F. Tokunaga, S. Fukai, Structures of CYLD USP with Met1- or Lys63-linked diubiquitin reveal mechanisms for dual specificity, Nat. Struct. Mol. Biol. 22 (2015) 222–229.
[93] D.P. Dowlatshahi, V. Sandrin, S. Vivona, T.A. Shaler, S.E. Kaiser, F. Melandri, W. I. Sundquist, R.R. Kopito, ALIX is a Lys63-specific polyubiquitin binding protein that functions in retrovirus budding, Dev. Cell 23 (2012) 1247–1254.
[94] A. Lokapally, H. Neuhaus, J. Herfurth, T. Hollemann, Interplay of TRIM2 E3 ubiquitin ligase and ALIX/ESCRT complex: control of developmental plasticity during early neurogenesis, Cells 9 (2020).
[95] E. Lauwers, C. Jacob, B. Andre, K63-linked ubiquitin chains as a specific signal for protein sorting into the multivesicular body pathway, J. Cell Biol. 185 (2009) 493–502.
[96] Z. Erpapazoglou, O. Walker, R. Haguenauer-Tsapis, Versatile roles of k63-linked ubiquitin chains in trafficking, Cells 3 (2014) 1027–1088.
[97] H. Tanno, M. Komada, The ubiquitin code and its decoding machinery in the endocytic pathway, J. Biochem. 153 (2013) 497–504.
[98] M. Balastik, F. Ferraguti, A. Pires-da Silva, T.H. Lee, G. Alvarez-Bolado, K.P. Lu, P. Gruss, Deficiency in ubiquitin ligase TRIM2 causes accumulation of neurofilament light chain and neurodegeneration, Proc. Natl. Acad. Sci. U. S. A. 105 (2008) 12016–12021.
[99] P. Liu, W. Gan, S. Su, A.V. Hauenstein, T.M. Fu, B. Brasher, C. Schwerdtfeger, A. C. Liang, M. Xu, W. Wei, K63-linked polyubiquitin chains bind to DNA to facilitate DNA damage repair, Sci. Signal. 11 (2018).
[100] P.M. Lombardi, S. Haile, T. Rusanov, R. Rodell, R. Anoh, J.G. Baer, K.A. Burke, L. N. Gray, A.R. Hacker, K.R. Kebreau, C.K. Ngandu, H.A. Orland, E. Osei-Asante, D. P. Schmelyun, D.E. Shorb, S.H. Syed, J.M. Veilleux, A. Majumdar, N. Mosammaparast, C. Wolberger, The ASCC2 CUE domain in the ALKBH3-ASCC DNA repair complex recognizes adjacent ubiquitins in K63-linked polyubiquitin, J. Biol. Chem. 298 (2022), 101545.
[101] D. Srivastava, O. Chakrabarti, Mahogunin-mediated alpha-tubulin ubiquitination via noncanonical K6 linkage regulates microtubule stability and mitotic spindle orientation, Cell Death Dis. 5 (2014), e1064.
[102] F. Stegmeier, M.E. Sowa, G. Nalepa, S.P. Gygi, J.W. Harper, S.J. Elledge, The tumor suppressor CYLD regulates entry into mitosis, Proc. Natl. Acad. Sci. U. S. A. 104 (2007) 8869–8874.
[103] G. Liu, X. Wei, R. Chen, H. Zhou, X. Li, Y. Sun, S. Xie, Q. Zhu, N. Qu, G. Yang, Y. Chu, H. Wu, Z. Lan, J. Wang, Y. Yang, X. Yi, A novel mutation of the SLC25A13 gene in a Chinese patient with citrin deficiency detected by target next-generation sequencing, Gene 533 (2014) 547–553.
[104] M. Bai, Y. Che, K. Lu, L. Fu, Analysis of deubiquitinase OTUD5 as a biomarker and therapeutic target for cervical cancer by bioinformatic analysis, PeerJ 8 (2020), e9146.
[105] D. Iglesias-Gato, Y.C. Chuan, N. Jiang, C. Svensson, J. Bao, I. Paul, L. Egevad, B. M. Kessler, P. Wikstrom, Y. Niu, A. Flores-Morales, OTUB1 de-ubiquitinating enzyme promotes prostate cancer cell invasion in vitro and tumorigenesis in vivo, Mol. Cancer 14 (2015) 8.
[106] P. Giannakakou, D.L. Sackett, Y. Ward, K.R. Webster, M.V. Blagosklonny, T. Fojo, p53 is associated with cellular microtubules and is transported to the nucleus by dynein, Nat. Cell Biol. 2 (2000) 709–717.
[107] N.D. Marchenko, W. Hanel, D. Li, K. Becker, N. Reich, U.M. Moll, Stress-mediated nuclear stabilization of p53 is regulated by ubiquitination and importin-alpha3 binding, Cell Death Differ. 17 (2010) 255–267.
[108] M. Akutsu, Y. Ye, S. Virdee, J.W. Chin, D. Komander, Molecular basis for ubiquitin and ISG15 cross-reactivity in viral ovarian tumor domains, Proc. Natl. Acad. Sci. U. S. A. 108 (2011) 2228–2233.
[109] D. Schluter, E. Schulze-Niemand, M. Stein, M. Naumann, Ovarian tumor domain proteases in pathogen infection, Trends Microbiol. 30 (2022) 22–33.
[110] J. Sires-Campos, A. Lambertos, C. Delevoye, G. Raposo, D.C. Bennett, E. Sviderskaya, C. Jimenez-Cervantes, C. Olivares, J.C. Garcia-Borron, Mahogunin ring finger 1 regulates pigmentation by controlling the pH of melanosomes in melanocytes and melanoma cells, Cell. Mol. Life Sci. 79 (2021) 47.
[111] E. Bier, E.M.De Robertis, EMBRYO DEVELOPMENT. BMP gradients: A paradigm for morphogen-mediated developmental patterning, Science 348 (2015), aaa5838.
[112] M.E. Bronner, M. Simoes-Costa, The neural crest migrating into the twenty-first century, Curr. Top. Dev. Biol. 116 (2016) 115–134.
[113] C. Niehrs, Head in the WNT: the molecular nature of Spemann's head organizer, Trends Genet. 15 (1999) 314–319.
[114] W. Li, A. Yao, H. Zhi, K. Kaur, Y.C. Zhu, M. Jia, H. Zhao, Q. Wang, S. Jin, G. Zhao, Z.Q. Xiong, Y.Q. Zhang, Angelman syndrome protein Ube3a regulates synaptic growth and endocytosis by inhibiting BMP signaling in drosophila, PLoS Genet. 12 (2016), e1006062.
[115] J.H. Chai, D.P. Locke, J.M. Greally, J.H. Knoll, T. Ohta, J. Dunai, A. Yavor, E. E. Eichler, R.D. Nicholls, Identification of four highly conserved genes between breakpoint hotspots BP1 and BP2 of the Prader-Willi/Angelman syndromes deletion region that have undergone evolutionary transposition mediated by flanking duplicons, Am. J. Hum. Genet. 73 (2003) 898–925.
[116] H.T. Tsang, T.L. Edwards, X. Wang, J.W. Connell, R.J. Davies, H.J. Durrington, C. J. O'Kane, J.P. Luzio, E. Reid, The hereditary spastic paraplegia proteins NIPA1, spastin and spartin are inhibitors of mammalian BMP signalling, Hum. Mol. Genet. 18 (2009) 3805–3821.
[117] K. Murakami, J.D. Etlinger, Role of SMURF1 ubiquitin ligase in BMP receptor trafficking and signaling, Cell. Signal. 54 (2019) 139–149.
[118] M.L. Piacentino, M.E. Bronner, Intracellular attenuation of BMP signaling via CKIP-1/Smurf1 is essential during neural crest induction, PLoS Biol. 16 (2018), e2004425.
[119] L. Herhaus, M.A. Al-Salihi, K.S. Dingwell, T.D. Cummins, L. Wasmus, J. Vogt, R. Ewan, D. Bruce, T. Macartney, S. Weidlich, J.C. Smith, G.P. Sapkota, USP15 targets ALK3/BMPR1A for deubiquitylation to enhance bone morphogenetic protein signalling, Open Biol. 4 (2014), 140065.
[120] M. Inui, A. Manfrin, A. Mamidi, G. Martello, L. Morsut, S. Soligo, E. Enzo, S. Moro, S. Polo, S. Dupont, M. Cordenonsi, S. Piccolo, USP15 is a deubiquitylating enzyme for receptor-activated SMADs, Nat. Cell Biol. 13 (2011) 1368–1375.
[121] W.K. Tse, Y.J. Jiang, C.K. Wong, Zebrafish transforming growth factor-beta-stimulated clone 22 domain 3 (TSC22D3) plays critical roles in bmp-dependent dorsoventral patterning via two deubiquitylating enzymes Usp15 and Otud4, Biochim. Biophys. Acta 2013 (1830) 4584–4593.
[122] F. Zhou, F. Xie, K. Jin, Z. Zhang, M. Clerici, R. Gao, M. van Dinther, T.K. Sixma, H. Huang, L. Zhang, P. Ten Dijke, USP4 inhibits SMAD4 monoubiquitination and promotes activin and BMP signaling, EMBO J. 36 (2017) 1623–1639.